Structural transition of various-sized sphere-platelet mixtures

Akiho Tani,[1] Yutaro Tanii,[1] Kyoka Ishiyama,[1] Shusaku Harada,[1,*] and Hisao Satoh[2]
[1]*Faculty of Engineering, Hokkaido University, N13-W8 Sapporo, Hokkaido 060-8628, Japan*
[2]*Japan Nuclear Fuel Limited, 504-22 Nozuki, Obuchi, Rokkasho, Aomori 039-3212, Japan*

(Received 18 October 2021; accepted 15 March 2022; published 5 April 2022)

Monte Carlo simulations on the structural change of hard sphere-platelet mixtures were performed to investigate the effect of particle size. We quantitatively analyzed local equilibrium structures of sphere-platelet mixtures with varying size ratios under various sphere and platelet density conditions. Based on the simulation results, we investigated the structural transitions such as isotropic to anisotropic, clustering, and so on. When a small amount of small-sized sphere is added to a large-sized platelet system, the mixture structure transitions from isotropic to nematic ones as the platelet number density increases. On the other hand, the platelet forms clusters with the addition of a large number of spheres. In a small platelet–large sphere system, the spheres form aggregates by increasing platelet density instead. The platelet and spherical particles exhibit different structural transitions depending on the size and density. In the limit of small and large size ratios, the structures of the platelet-sphere mixture obtained from the Monte Carlo simulation are close to those shown by previous theoretical and experimental studies, respectively. Because the primary actor shifts from sphere to platelet as the size ratio changes, the transition boundary shifts continuously. When the size ratio is close to unity, the most complicated behavior is observed, with both the platelet and sphere simultaneously acting the leading part.

DOI: 10.1103/PhysRevE.105.044602

I. INTRODUCTION

Colloidal particle mixtures with various sizes and shapes are common in many fields including geology, biology, and material sciences [1]. When different types of particles are mixed, they form a wide variety of inhomogeneous structures depending on mixture conditions due to the depletion effect [2,3]. Understanding the structure of particle mixtures for a given condition is essential for evaluating not only the mechanical properties of composite materials, but also the transport properties in them.

Several studies of different-shaped particle mixtures have been conducted with various systems such as sphere-platelet [4–9], rod-platelet [10], sphere-macromolecules [11,12], platelet-macromolecules [13], etc. In particular, sphere-platelet mixtures have been studied to understand clay particle structures. Clay particles, such as montmorillonite, have a platelike shape, as is well known [14]. Mixtures of clays with other colloidal particles have a wide variety of states and their properties, such as catalytic [15], optical [16], rheological or electric, and magnetic properties [17,18], vary depending on the mixture conditions. As a result, numerous studies of the structural change of sphere-platelet mixtures have been conducted. Oversteegen and Lekkerkerker [4] investigated the structural transition of large sphere–small platelet mixtures by free volume theory with the equation of state of the mixture system. They discovered that by adding a small amount of platelet, the mixture structure changes dramatically. Kleshchanok *et al.* [6] experimentally investigated the structural change of gibbsite-silica mixtures. They observed that disk-shaped large gibbsite particles form aggregates by adding small spherical-shaped silica particles. Although the particle size influences these behaviors of sphere-platelet mixtures, previous studies examined them under specific particle size conditions. The structures of sphere-platelet mixtures are expected to be sensitive to size and density conditions.

In this study, the structural change of rigid-body sphere-platelet mixtures was investigated. We obtained local equilibrium structures of mixtures by Monte Carlo simulation under various size and density conditions. From the simulation results, we quantified the structures of sphere and platelet in the mixtures, i.e., isotropic or anisotropic (nematic), homogeneous or inhomogeneous, clustering or nonclustering, and so on. We focused on the local clustering of both particles by the depletion effect, which can be the onset of thermodynamic phase separation. Particularly, we examined how the density and the size of each particle influences the overall structure of a sphere-platelet system. We compared the mixture structures obtained from the simulation with those reported by previous studies.

II. SIMULATION METHOD

The equilibrium structures of the sphere-platelet binary system were computed by Monte Carlo simulation. We assumed infinitely thin disk particles with diameter σ and monodispersed spherical particles with a diameter σ_S. The size ratio σ/σ_S is an important parameter in this study. The simulation conditions were modified in accordance with the size ratio. When the sphere was larger than the platelet,

*harada@eng.hokudai.ac.jp

the number of spheres, N_S, was fixed while the number of platelets, N, was changed. We set $N_S = 100$ for $\sigma/\sigma_S = 0.4$ and 0.67, and $N_S = 200$ (or $N_S = 50$ in one case) for $\sigma/\sigma_S = 1.0$, respectively. In cases where the sphere was smaller than the platelet, the number of platelets was fixed as $N = 3000$ for $\sigma/\sigma_S = 1.5$ and $N = 2160$ for $\sigma/\sigma_S = 5.0$, while the number of spheres, N_S, was changed.

The calculation region was cubic, with L being a variable side length. The periodic boundary conditions were applied in all directions. The particles were arranged in the initial configuration by using a random number to set the position vector of the sphere and platelet as well as the normal vector of the platelet. We assumed the rigid-body potential for both sphere and platelet interparticle potentials. The geometric calculation was conducted to check the intersection of each particle in order to avoid particle overlap. By changing the position and orientation of a certain particle, each Monte Carlo step was completed. The maximum displacement per translation is $\Delta r = 0.02\sigma$ for the platelet and $0.02\sigma_S$ for the sphere, respectively. The maximum variation for the normal vector component of the platelet is set to be $\Delta v = 0.02$ [19].

To obtain the equilibrium structure of platelet-sphere mixtures, we performed an NPT Monte Carlo simulation [20]. Under the assumption of constant pressure, the volume of the calculation region, $V(= L^3)$, was changed. We keep the size of the calculation region more than 4σ. The equilibrium structure of the system was iteratively determined by whether the volume of the calculation region reached a constant value for a given pressure, along with the convergence of some parameters describing particle configurations, as explained below. In Monte Carlo (MC) simulations, we calculated 50 000 MC steps per one particle (both sphere and platelet) at least, and 300 000 MC steps per one particle at a maximum.

As explained later, the structural transition was judged by some configurational parameters that describe the particle structures such as the nematic order parameter. This judgment does not strictly reflect a thermodynamic phase transition. As suggested in the previous study [21], it is difficult to precisely obtain the phase behaviors of a binary system by NPT Monte Carlo simulation. Therefore, we only discuss the local structural change of each particle by the depletion effect from the results of MC simulation assuming a finite calculation region. For this reason, we do not use the term "phase" in this study.

However, we observed that the structural change causes a change in the thermodynamic relation. As an example, Fig. 1 shows the relation between nondimensional pressure $p\sigma^3/k_BT$ and reciprocal of volume $1/V$ obtained from NPT Monte Carlo simulation for $\sigma/\sigma_S = 1.5$, $N = 3000$, and $N_S = 250$ and 750. As can be seen in the figure, the thermodynamic relation (density-pressure relation in this case) changes discontinuously when the equilibrium structure changes, such as the isotropic-nematic transition of platelets or clustering of spheres, which are quantitatively explained in the later part. As mentioned above, it does not correspond to thermodynamic phase transitions in a binary system of hard particles, which requires more complicated simulation protocols [22]. However, these results indirectly imply that the structural change corresponds to the thermodynamic phase transition in some cases.

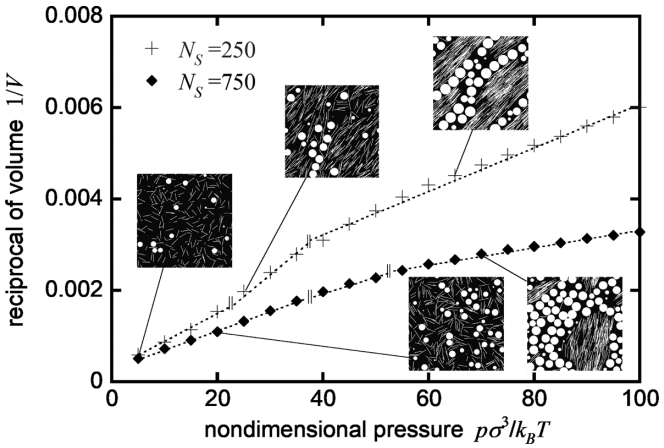

FIG. 1. Relation between nondimensional pressure and reciprocal of volume of the platelet-sphere system for $\sigma/\sigma_S = 1.5$, $N = 3000$, and $N_S = 250$ and 750.

III. RESULTS AND DISCUSSION

A. Large sphere–small platelet system

Figure 2 shows the equilibrium structures of sphere-platelet mixtures obtained from Monte Carlo simulation for $\sigma/\sigma_S = 0.4$. Figure 2(a) illustrates three-dimensional (3D) snapshots of the particle structure and their partial sectional views. We chose these configurations for an almost constant volumetric fraction of the sphere ($\phi \sim 0.24$) from simulation results for the different number of spheres, N_S. The platelet

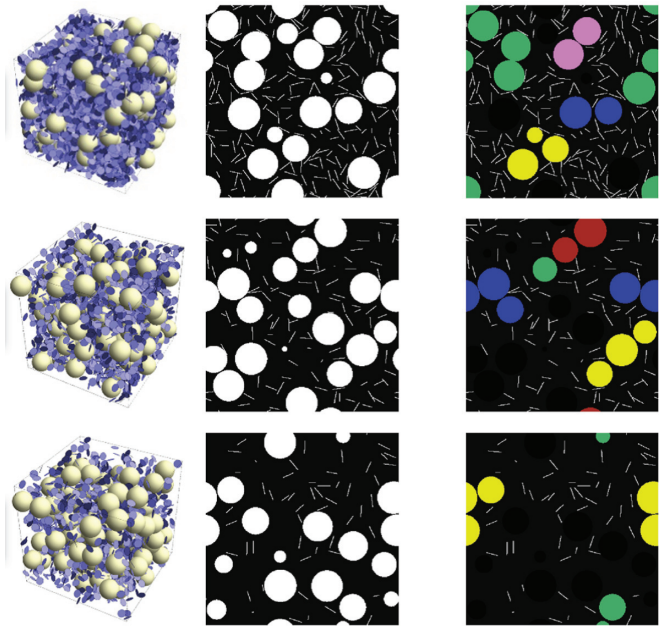

(a) 3D and 2D structures (b) cluster

FIG. 2. Snapshots of typical configurations of small platelet–large sphere mixtures at $\sigma/\sigma_S = 0.4$ and $\phi \sim 0.24$. (a) 3D snapshots and their partial sectional views for platelet nondimensional density $N\sigma^3/V = 1.19$ (upper), 0.60 (middle), and 0.29 (lower). (b) Spheres coaggregated as clusters (colored).

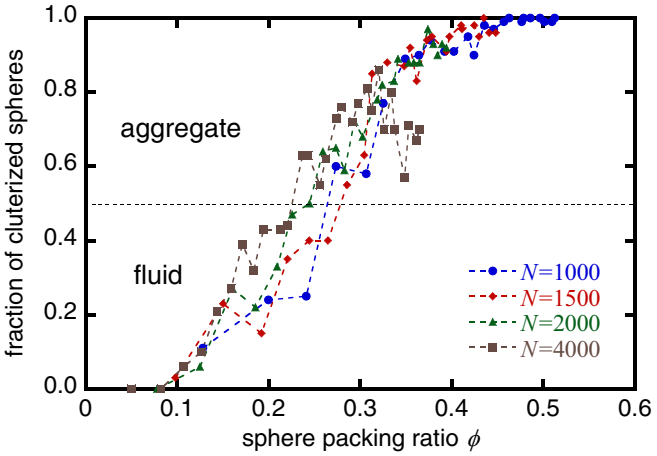

FIG. 3. Fraction of clusterized spheres as functions of sphere volume fraction ϕ at $\sigma/\sigma_S = 0.4$ for number of platelet $N = 1000$, 1500, 2000, and 4000.

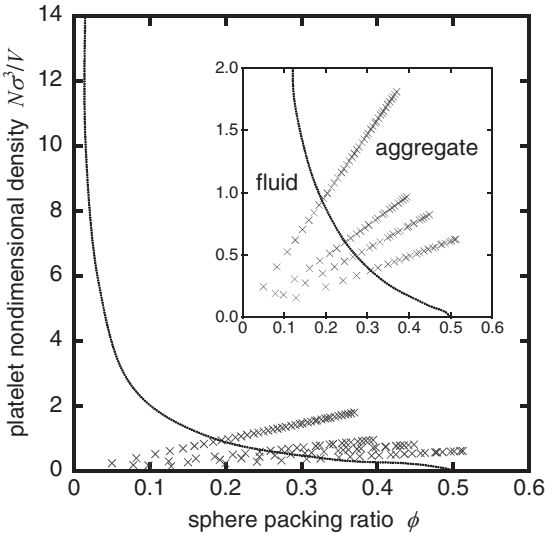

FIG. 4. Structural transition of small platelet–large sphere mixtures obtained from Monte Carlo simulation for $\sigma/\sigma_S = 0.4$. Dotted line indicates the transition boundary of the sphere.

nondimensional number density is $N\sigma^3/V = 1.19$ (upper), 0.60 (middle), and 0.29 (lower), respectively.

As the platelet density increases, the spheres approach each other and form a chainlike aggregate. This is due to the depletion effect caused by adding small platelets [3]. Figure 2(b) (right column) shows extracted sphere clusters for each condition. Spheres in the same group are painted with the same colors, while black spheres are isolated from others. In this study, we evaluated sphere clustering from interparticle distance, i.e., a cluster was formed when the distance of two spheres was less than 10% of the sphere diameter. At small platelet density (lower case), sphere clusters are rare, whereas most spheres belong to clusters at large platelet density (upper case). It is also found that the platelet configuration is isotropic in all cases because the platelet density is not as large as that which occurs in the isotropic-nematic transition, as explained further below.

Figure 3 shows the fraction of clusterized spheres at $\sigma/\sigma_S = 0.4$ for number of platelets $N = 1000$, 1500, 2000, and 4000. When the sphere packing ratio ϕ is small, the fraction remains low, but it suddenly increases with increasing ϕ. As ϕ exceeds 0.4, nearly all spheres belong to the cluster. The clustering occurs at a lower volume fraction ϕ for the larger number of platelets, N. Based on the results in Fig. 3, we determined that the structural change occurs when 50% of the spheres belong to any of the clusters, and classified both structures as "fluid" and "aggregate" ones. By our definition, the fluid structure describes that the sphere distributes almost uniformly, while the aggregate structure involves not only ordered or disordered aggregate but also chainlike clusters of spheres.

Figure 4 indicates the structural transition of sphere-platelet mixtures obtained from Monte Carlo simulation at $\sigma/\sigma_S = 0.4$. The cross plots indicate the conditions under which Monte Carlo simulation was performed. The lines formed by the cross symbols are the "trajectories" of NPT Monte Carlo simulation and therefore they have no physical meaning. A dotted line indicates the approximate transition boundary between fluid and aggregate structures of spheres, as determined by the results in Fig. 3. Because the computational cost limits the number of platelets in large sphere–small platelet mixtures, Monte Carlo simulation was performed only at small platelet density. The transition boundary for large platelet density is an expected line drawn by extrapolating the low platelet density data.

As illustrated in Fig. 4, the structural change from fluid to aggregate ones is affected by both the sphere packing ratio ϕ and the platelet number density $N\sigma^3/V$. Spheres make aggregates easily at larger sphere packing ratio by adding a small amount of platelet. As is well known, spheres crystallize regularly even in a monodispersed sphere system at the dense limit ($\phi \sim 0.5$) [23]. The structural transition of large sphere–small platelet mixtures obtained from Monte Carlo simulation is similar to those found in the previous study. Oversteegen *et al.* [4] theoretically examined the equilibrium structure of large sphere–small platelet mixtures by a scaled particle theory. Although it is estimated from the configurational cluster judgement depending on the definition of clusters, the boundary shown in Fig. 4 qualitatively agrees with that shown in their analysis.

These results show that the depletion effect causes structural changes in large spheres resulting from the addition of small platelets, even in dilute systems of sphere-platelet mixtures. On the other hand, the structural change of platelets was not observed within the range of our Monte Carlo simulation. The isotropic-nematic transition (IN transition) of a pure platelet system is known to occur around the platelet density $N\sigma^3/V \sim 4$–6 [24]. The platelet density is too dilute to detect the IN transition of platelets under the conditions shown in this section.

B. Small sphere–large platelet system

A Monte Carlo simulation of a small sphere–large platelet system was also performed. Also in this case, the mixture structures are affected by the density conditions of the sphere

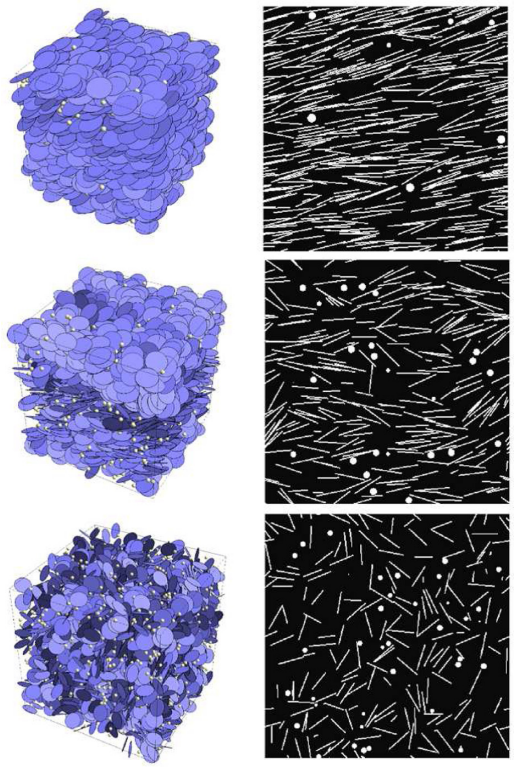

FIG. 5. 3D snapshots of typical configurations and partial sectional views of large platelet–small sphere mixtures at $\sigma/\sigma_S = 5.0$ and $\phi \sim 0.007$. Platelet nondimensional density $N\sigma^3/V = 9.89$ (upper), 5.04 (middle), and 2.60 (lower).

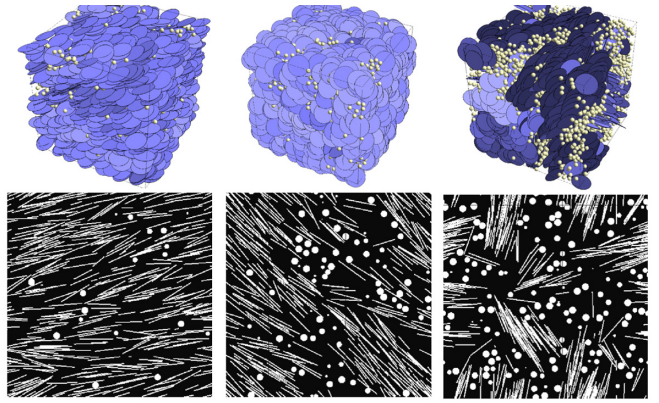

(a) 3D and 2D structures

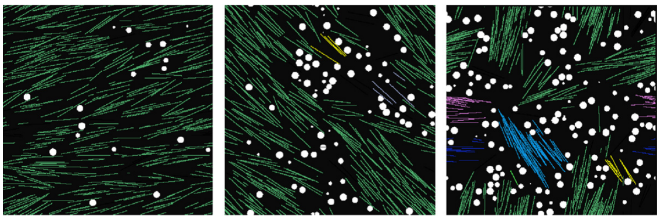

(b) cluster

FIG. 6. Snapshots of typical configurations and partial sectional views at $\sigma/\sigma_S = 5.0$ and $N\sigma^3/V \sim 9.0$ for sphere packing ratio $\phi = 0.013$ (left), 0.038 (center), and 0.076 (right).

and platelet. Figure 5 indicates the mixture structures of a small sphere–large platelet system with $\sigma/\sigma_S = 5.0$ for small sphere packing ratio ($\phi \sim 0.007$). The platelet nondimensional density is $N\sigma^3/V = 9.89$ (upper), 5.04 (middle), and 2.60 (lower), respectively. As shown in Fig. 5, the platelet distributes isotropically at small density and exhibits nematic structures as the density increases. This structural change is similar to the IN transition in a pure platelet system, which occurs at $N\sigma^3/V \sim 4$–6. Although the presence of sphere disrupts the nematic structure of the platelet, the IN transition can be observed around the IN boundary of a pure platelet system if the sphere packing ratio is relatively small.

Next we consider the structural change of large platelets by adding small spheres. Figure 6(a) shows 3D snapshots and cross-sectional views of the mixture structures in a small sphere–large platelet system with $\sigma/\sigma_S = 5.0$ for the platelet density $N\sigma^3/V \sim 9.0$. As shown in Fig. 6, when the sphere packing ratio is small (left case), the platelet forms nematic structures because the platelet density exceeds the IN boundary of the platelet system. On the other hand, when the sphere packing ratio is large (right case), the platelet forms clusters by adding small spheres. Obviously, the clustering of the large platelet results from the depletion effect. The similar clustering of the platelet was observed in the experiments of a gibbsite-silica system [6].

Figure 6(b) illustrates the results of the extraction of platelet clusters from the configurations shown in Fig. 6(a). The platelets with the same color indicate that they belong to the same cluster. The clustering of the platelet was judged by the following procedure [25]. First, we calculated the correlation factor of platelet orientation c at the position of each platelet $\boldsymbol{r}_i$ by the Gaussian weight function as follows:

$$c(\boldsymbol{r}_i) = \sum_{j \neq i}^{N} \exp\left[-\frac{(\boldsymbol{r}_i - \boldsymbol{r}_j)^2}{2\lambda^2}\right] \boldsymbol{u}_i \cdot \boldsymbol{u}_j, \tag{1}$$

where $\boldsymbol{r}_i$, $\boldsymbol{r}_j$ is the position vector of the platelet, $\boldsymbol{u}_i$, $\boldsymbol{u}_j$ is the normal vector of the platelet, and λ is the Gaussian parameter. The platelet with a large value of $c(\boldsymbol{r}_i)$ was considered as the candidate of the central platelet of the cluster. The platelets in each cluster were judged if the following conditions were satisfied:

$$(\boldsymbol{r}_i - \boldsymbol{r}_j)^2 < \gamma_{pc}, \tag{2}$$

$$|\boldsymbol{u}_i \cdot \boldsymbol{u}_j| < \delta_{pc}. \tag{3}$$

The former condition [Eq. (2)] seeks platelets with nearby neighbors (small interparticle distance) and the latter [Eq. (3)] seeks platelets that are aligned (similar orientation). We used the parameters $\gamma_{pc} = \sigma/2$ (σ: platelet diameter) and $\delta_{pc} = 0.94$, respectively. As shown in Fig. 6(b), if the sphere packing ratio is small, almost all platelets belong to the same cluster. On the other hand, platelet clusters are divided into many parts by increasing the sphere packing ratio.

Figure 7 shows the rate of platelets belonging to clusters as functions of the platelet nondimensional density $N\sigma^3/V$ for $\sigma/\sigma_S = 5.0$. As shown in Fig. 7, the platelet clustering increases as platelet density increases. Almost all platelets belong to any clusters under the condition of $N\sigma^3/V > 8.0$.

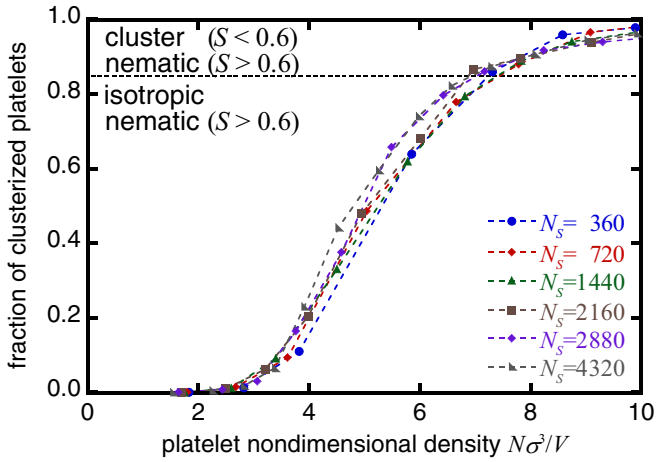

FIG. 7. Fraction of clusterized platelets as functions of platelet nondimensional density $N\sigma^3/V$ for $\sigma/\sigma_S = 5.0$.

However, as indicated in Fig. 6 (left or center), the platelets form a single large cluster in some cases, which should be classified as nematic structures. Therefore, we classified isotropic, nematic, and cluster structures also by nematic order parameter S as

$$S = \frac{1}{N}\sum_{i=1}^{N}\left[\frac{3}{2}(\boldsymbol{n}\cdot\boldsymbol{u}_i)^2 - \frac{1}{2}\right], \tag{4}$$

where $\boldsymbol{n}$ is the nematic director vector. Figure 8 shows the nematic order parameter of the platelet for $\sigma/\sigma_S = 5.0$. When a small amount of sphere is added, the nematic order parameter increases at $N\sigma^3/V \sim 4$–6 (IN boundary), whereas it keeps a small value when the number of spheres is large. This is because the clustering prevents platelets from aligning in the same direction, which is shown in Fig. 6 (right). We classified platelet structures using both the fraction of clusterized platelets and nematic order parameters. Generally, the IN transition of an infinitely thin platelet system is judged by the rapid increase of the nematic order parameter S [24]; for example, whether or not S exceeds 0.5. However, the

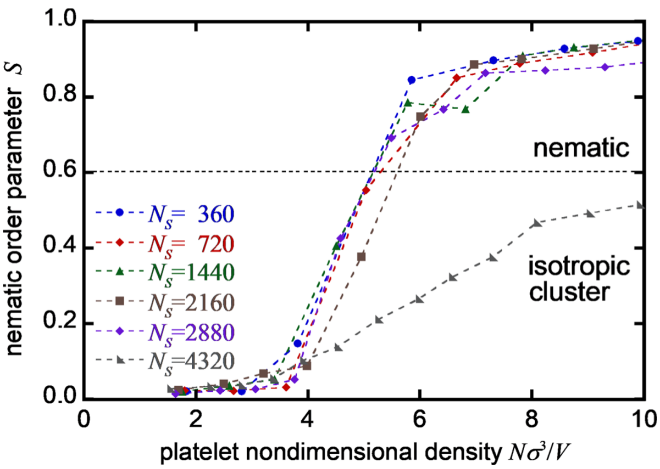

FIG. 8. Nematic order parameter of platelet as functions of platelet nondimensional density $N\sigma^3/V$ for $\sigma/\sigma_S = 5.0$.

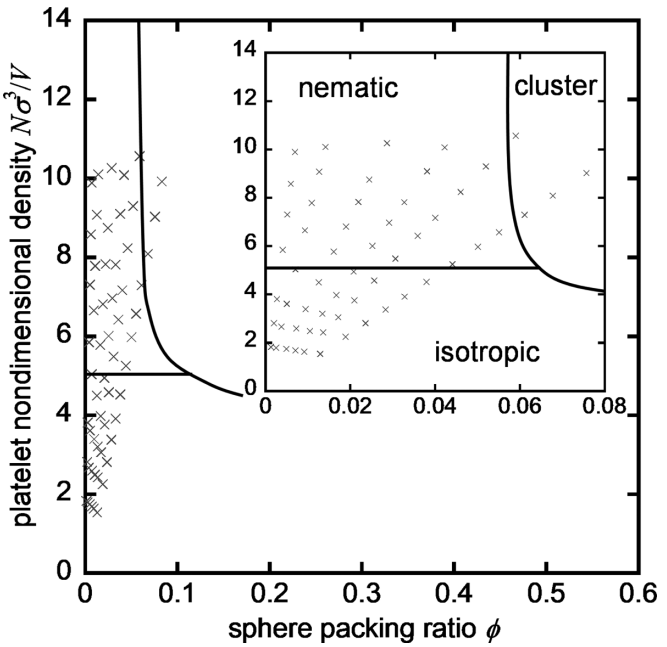

FIG. 9. Structural transition of platelet-sphere mixtures obtained from Monte Carlo simulation for $\sigma/\sigma_S = 5.0$.

transition of nematic to cluster structures has to be judged simultaneously. Obviously, the platelet structure shown in Fig. 6 should be classified as "cluster" ones; nevertheless, the nematic order parameter value exceeds 0.5, as shown in Fig. 8. Therefore, we judged the platelet structure on the basis of the results shown in Figs. 6 and 8. The structural change from isotropic to nematic ones occurs if the nematic order parameter S exceeds 0.6. Furthermore, we considered as the cluster structure if 85% of platelets belong to any clusters and the nematic order parameter S does not exceed 0.6.

Figure 9 shows the structural transition of sphere-platelet mixtures for $\sigma/\sigma_S = 5.0$. The solid lines indicate the approximate transition boundary evaluated from the simulation results. The structural change of a small sphere–large platelet system totally differs from that of a large sphere–small platelet system, as illustrated in Fig. 4. The number of spheres greatly influences the platelet structure. When the sphere packing ratio exceeds a specific value at moderate to dense platelet conditions, the platelet forms clusters. These structural changes are very similar to those observed in the experiment with gibbsite (large platelet) and silica particles (small sphere) [6].

C. Sphere-platelet system of comparable size

As previously explained, the depletion effect results in clustering of large particles in a binary mixture system. We also examined the mixture structure of a sphere-platelet system of comparable size by Monte Carlo simulation. Figure 10(a) indicates snapshots of typical structures of platelet-sphere mixtures for $\sigma/\sigma_S = 1.5$. We choose the conditions in which the platelet number density is nearly constant ($N\sigma^3/V \sim 4.6$). The sphere packing ratio is $\phi = 0.060$ (left), 0.184 (center), and 0.362 (right) (number of spheres, N_S =250, 750, and 1500), respectively. As seen in these

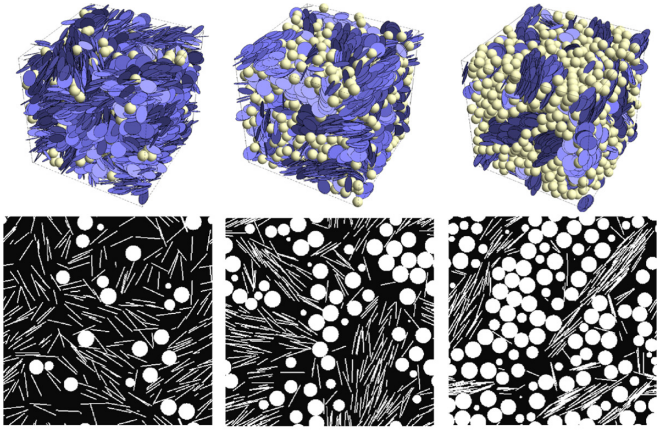

(a) 3D and 2D structures

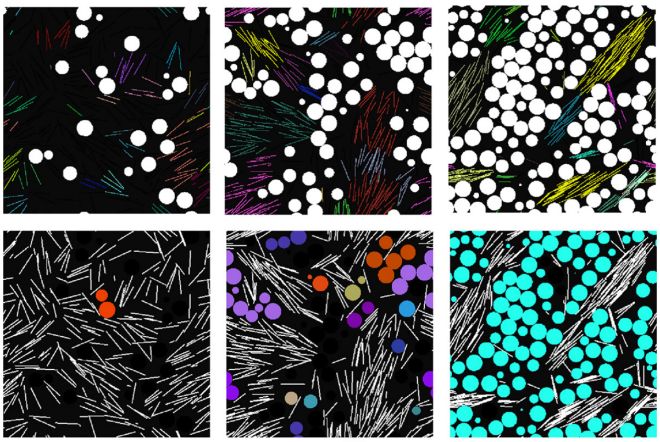

(b) cluster of platelet (upper) and sphere (lower)

FIG. 10. Snapshots of typical configurations and partial sectional views for $\sigma/\sigma_S = 1.5$ and $N\sigma^3/V \sim 4.6$. The sphere packing ratio is $\phi = 0.060$ (left), 0.184 (center), and 0.362 (right).

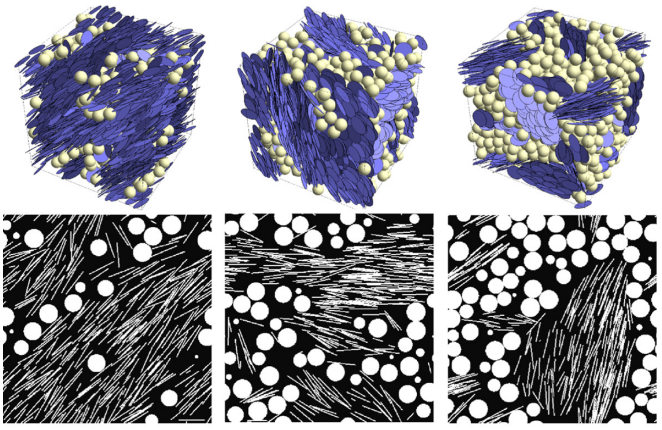

(a) 3D and 2D structures

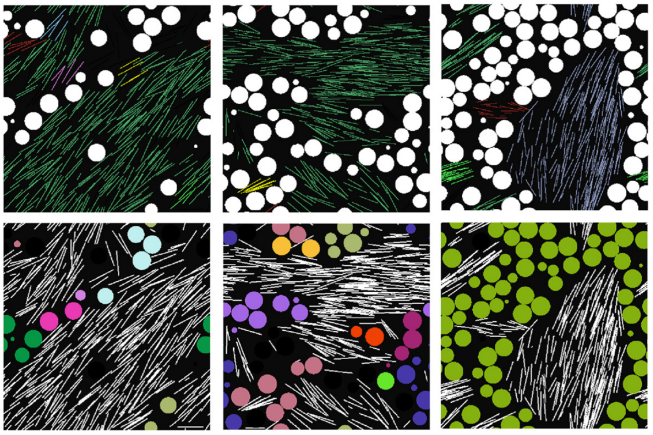

(b) cluster of platelet (upper) and sphere (lower)

FIG. 11. Snapshots of typical configurations and partial sectional views for $\sigma/\sigma_S = 1.5$ and $N\sigma^3/V \sim 7.2$. The sphere packing ratio is $\phi = 0.094$ (left), 0.189 (center), and 0.288 (right).

structures, sphere-platelet mixtures of similar sizes exhibit complicated structures depending on the density condition.

Figure 10(b) indicates the results of the cluster judgment of the platelet (upper) and sphere (lower), respectively. As the sphere packing ratio increases, most of the spheres and platelets form clusters. When the platelet and sphere sizes are comparable in size, both particles exhibit complex clustering behaviors depending on the density conditions. At low sphere packing ($\phi = 0.060$), the spheres exist almost uniformly (fluid phase). Then both the sphere and platelet form clusters at moderate sphere packing condition ($\phi = 0.184$). At dense sphere packing ($\phi = 0.362$), the spheres form a large cluster by the surrounding platelet clusters.

The structure becomes more complicated as the platelet density increases. Figure 11(a) indicates the structure of platelet-sphere mixtures for $\sigma/\sigma_S = 1.5$ and $N\sigma^3/V \sim 7.2$. The sphere packing fraction is $\phi = 0.094$ (left), 0.189 (center), and 0.288 (right) (number of sphere, $N_S = 250$, 500, and 750), respectively. At low sphere packing ratio, the platelet exhibits divided nematic structures in which it is aligned almost in parallel. As the sphere increases, the platelets are separated into clusters by the surrounding sphere networks. Figure 11(b) indicates platelet and sphere clusters, respectively. In a binary system of comparable size, the leading role frequently changes, i.e., one particle makes network structures at the edges of the clusters of the other particles.

Based on the results of the cluster judgment shown in Figs. 10 and 11, we classify the structure of the platelets and spheres in mixtures of comparable size. Figure 12 shows the structural transition of the platelet-sphere mixture for $\sigma/\sigma_S = 1.5$. The transition boundaries are approximately drawn from the cluster judgment results with the same threshold values for sphere and platelet clusters as explained in the previous sections. The dotted line in Fig. 12 indicates the boundary of the sphere structure. The region with a small sphere packing ratio corresponds to the fluid structure, while the region with a large packing ratio is the aggregate one. The solid lines indicate the boundary of the platelet structure between isotropic, nematic, and cluster. As shown in Fig. 12, mixtures of comparable size exhibit complicated structural transitions due to the combination of sphere and platelet clustering.

We compared the simulation results of platelet-sphere structures of comparable sizes to the observation results of a similar binary system. The inset images in Fig. 12 indicate images of montmorillonite-zeolite structures obtained via 3D-XCT scanning. In the experiment, the montmorillonite

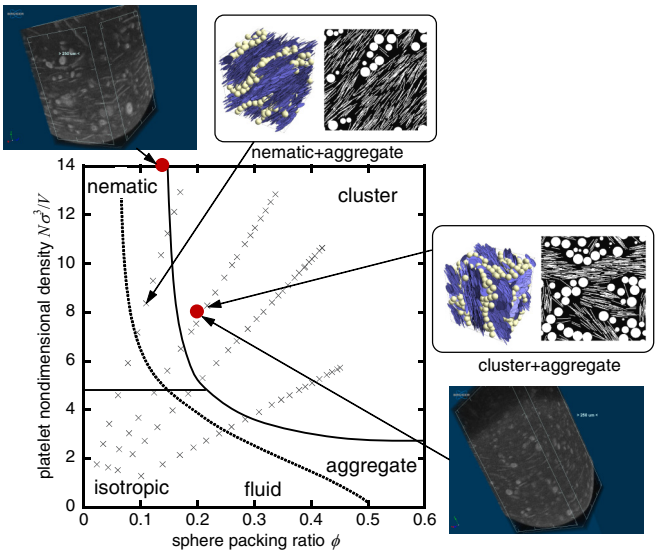

FIG. 12. Structural transition of platelet-sphere mixtures obtained from Monte Carlo simulation for $\sigma/\sigma_S = 1.5$. Dotted line and solid lines indicate the transition boundary of the sphere and platelet, respectively. Inset pictures are X-ray computed tomography (XCT) images of montmorillonite and zeolite mixtures.

particle has a platelet shape with an average diameter of $\sigma = 320$ nm and a thickness of 1 nm. The zeolite particle has a spherical shape and has an average diameter of $\sigma_S = 200$ nm. The density of these particles is 2700 kg/m^3 (montmorillonite) and 2120 kg/m^3 (zeolite), respectively. The size ratio of the platelet and sphere is $\sigma/\sigma_S = 1.6$. The 3D-XCT images were obtained under two density conditions, as indicated by the red plots in Fig. 12. As shown in these images, the structures obtained from the Monte Carlo simulation are similar to the observations in the actual binary system. When the sphere packing ratio is small and the platelet density is large (upper left image), the XCT image shows a nematic-aggregate structure, i.e., the platelets are aligned in one direction and the spheres concentrate partially. The XCT image of a large sphere packing ratio (lower right image) shows a cluster-aggregate structure in which the spheres form networks in isolated nematic structures of platelets. Although the comparison of the simulation results with experimental observation shown here is qualitative, it indicates that the clustering of the sphere and platelet causes the complicated structural change in the actual binary system.

D. Structural transition of sphere-platelet system

Figure 13 shows the structural transitions of platelet-sphere mixtures with various size ratios obtained from the Monte Carlo simulation. The transition boundaries are represented in each figure by solid lines for the platelet and dotted lines for the sphere. They are approximately drawn based on the simulation results or these extrapolations. As previously stated, the platelet-sphere mixtures at a small size ratio ($\sigma/\sigma_S = 0.4$, indicated in the leftmost figure) are composed of isotropic and nematic structures for the platelet and fluid and aggregate ones for the sphere. It is consistent with the theoretical prediction by scaled particle theory [4]. For the large size ratio ($\sigma/\sigma_S = 5.0$, in the rightmost figure), the mixture shows isotropic, nematic, and cluster structures for the platelet and fluid and aggregate ones for the sphere. It coincides with the experimental observation of a large platelet–small sphere system [6]. At moderate size ratio conditions, the transition boundary shifts continuously as the size ratio is changed.

As shown in Fig. 13, the structural change of the binary system is much more complicated than that of the single-particle system, particularly at a moderate size ratio. This is because the depletion effect reveals itself in a complicated manner and its leading role in the binary system frequently changes. Figure 14 indicates typical configurations of the platelet-sphere system obtained from the Monte Carlo simulation in the present study. The depletion effect and the nematic effect of the platelet bring about a wide variety of the structures in the binary system.

The particle clustering resulting from the depletion effect would be the onset of the thermodynamic phase separation in a binary system of hard particles. The locally clusterized structures can be found during the phase separation process, where small clusters grow up to reach large sizes during equilibration, although it takes a very long time [21]. From a practical point of view, these structural changes result in the complex variation of pore structures in the mixture. As a consequence, it may affect the transport properties in composite materials such as permeability, diffusion coefficient, and electrical conductivity. For example, Schneider *et al.* [26] conducted permeability experiments of mudstone composed of clay and silt-sized silica, and examined the effect of the clay-silt ratio on the permeability. They reported that "silt bridges" in mudstone form large pores that serve as high permeability pathways. Knowing the structure of the different-shaped particle mixtures shown in Fig. 14 is important for the prediction and passive control of the transport phenomena in it.

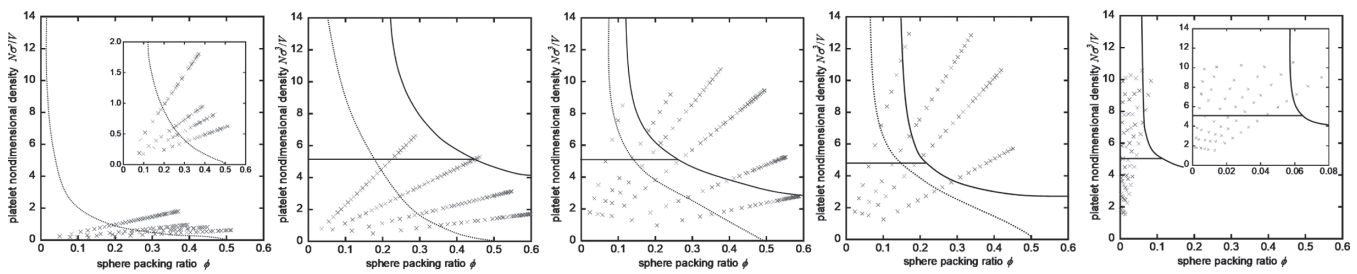

(a) $\sigma/\sigma_S = 0.4$ (b) $\sigma/\sigma_S = 0.67$ (c) $\sigma/\sigma_S = 1.0$ (d) $\sigma/\sigma_S = 1.5$ (e) $\sigma/\sigma_S = 5.0$

FIG. 13. Structural transition of platelet-sphere mixtures estimated from the results of a Monte Carlo simulation under various size ratios.

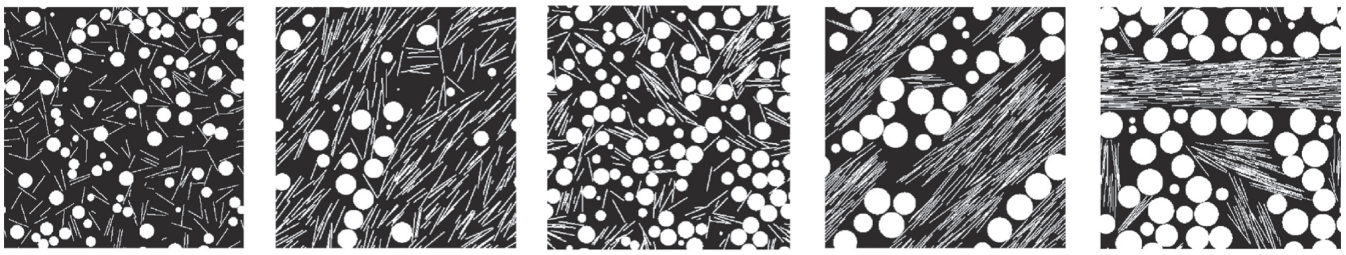

(a) I+F (b) N+F (c) I+Ag (d) N+Ag (e) Cl+Ag

FIG. 14. Typical structures of platelet-sphere mixtures. I: isotropic; N: nematic; and Cl: cluster, for platelet. F: fluid; Ag: aggregate, for sphere.

IV. CONCLUSIONS

The structural transition of hard sphere-platelet mixtures was investigated by Monte Carlo simulation under various size conditions. The structure of platelet and spherical particles was, respectively, classified by geometric characteristics such as the cluster formation ratio. Although such a structural change does not immediately reflect a thermodynamic phase transition, we confirmed that it may cause a change in the thermodynamic relation under certain conditions.

In a large sphere–small platelet system, the spheres form aggregates with increasing the platelet density due to the depletion effect. As a result, the sphere transitions from "fluid " to "aggregate" structures. The transition behaviors obtained from the Monte Carlo simulation are consistent with the theoretical prediction in the previous study.

In a small sphere–large platelet system, the platelet transitions from isotropic to nematic structures with increasing its density, which occurs even though no spheres are added (IN transition). By adding small spheres in a large platelet system, the platelet forms clusters due to the depletion effect. The transition from isotropic to nematic and cluster structures is similar to the experimental observations of large platelet (gibbsite)–small sphere (silica) mixtures.

Depending on the density conditions, a sphere-platelet system of comparable size exhibits complicated structural changes. The particles form chainlike aggregates at the edge of other particle clusters under certain conditions. Similar structures are also observed in XCT images of montmorillonite-zeolite mixtures of comparable size.

In this study, the structural transitions of sphere-platelet mixtures with varying size ratios were investigated. The transition boundary shifts continuously as the size ratio changes. The most complicated structural change is observed when the size ratio is close to unity. The structural change may affect the transport properties in particle mixtures such as permeability, as well as the diffusion coefficient of composite materials.

[1] W. B. Russel, D. A. Saville, and W. R. Schowalter, *Colloidal Dispersions* (Cambridge University Press, Cambridge, 1989).

[2] L. Onsager, Ann. NY Acad. Sci. **51**, 627 (1949).

[3] S. Asakura and F. Oosawa, J. Chem. Phys. **22**, 1255 (1954).

[4] S. M. Oversteegen and H. N. W. Lekkerkerker, J. Chem. Phys. **120**, 2470 (2004).

[5] S. M. Oversteegen, C. Vonk, J. E. G. J. Wijnhoven, and H. N. W. Lekkerkerker, Phys. Rev. E **71**, 041406 (2005).

[6] D. Kleshchanok, A. V. Petukhov, P. Holmqvist, D. V. Byelov and, H. N. Lekkerkerker, Langmuir **26**, 13614 (2010).

[7] N. Doshi, G. Cinacchi, J. S. van Duijneveldt, T. Cosgrove, S. W. Prescott, I. Grillo, J. Phipps, and D. I. Gittins, J. Phys.: Condens. Matter **23**, 194109 (2011).

[8] J. Landman, E. Paineau, P. Davidson, I. Bihannic, L. J. Michot, A.-M. Philippe, A.V. Petukhov, and H. N. W. Lekkerkerker, J. Phys. Chem. B **118**, 4913 (2014).

[9] S. Mo, X. Shao, Y. Chen, and Z Cheng, Sci. Rep. **6**, 36836 (2016).

[10] A. Galindo, A. J. Haslam, S. Verga, G. Jackson, A. G. Vanakaras, and D. A. Dunmur, J. Chem. Phys. **119**, 5216 (2003).

[11] E. H. A. de Hoog, W. K. Kegel, A. van Blaaderen, and H. N. W. Lekkerkerker, Phys. Rev. E **64**, 021407 (2001).

[12] R. Tuinier, J. Rieger, and C. G. de Kruif, J. Colloid Interface Sci. **103**, 1 (2003).

[13] S.-D. Zhang, P. A. Reynolds, and J. S. van Duijneveldt, J. Chem. Phys. **117**, 9947 (2002).

[14] L. Bailey, H. N. Lekkerkerker, and G. C. Maitland, Soft Matter **11**, 222 (2015).

[15] K. Mogyorosi, I. Dekany, and J. H. Fendler, Langmuir **19**, 2938 (2003).

[16] N. Miyamoto, H. Iijima, H. Ohkubo, and Y. Yamauchi, Chem. Commum. **46**, 4066 (2010).

[17] Y. F. Lan and J. J. Lin, J. Phys. Chem. A **113**, 8654 (2009).

[18] C. Galindo-Gonzalez, J. de Vicente, M. M. Ramos-Tejada, M. T. Lopez-Lopez, F. Gonzalez-Caballero, and J. D. G. Duran, Langmuir **21**, 4410 (2005).

[19] K. Terada, A. Tani, S. Harada, H. Satoh, and D. Hayashi, Mater. Res. Express **6**, 035514 (2018).

[20] D. Frenkel, and B. Smit, *Understanding Molecular Simulation from Algorithms to Applications* (Academic Press, San Diego, 2001).

[21] F. Gamez, R. D. Acemel, and A. Cuetos, Mol. Phys. **111**, 3136 (2013).

[22] A. Patti, and A. Cuetos, Mol. Sim. **44**, 516 (2018).

[23] B. J. Alder and T. E. Wainwright, J. Chem. Phys. **27**, 1208 (1957).

[24] R. Eppenga and D. Frenkel, Mol. Phys. **52**, 1303 (1984).

[25] A. Wouterse, S. R. Williams and, A. P. Philipse, J. Phys.: Condens. Matter **19**, 406125 (2007).

[26] J. Schneider, P. B. Flemings, R. J. Day-Stirrat, and J. T. Germaine, Geology **39**, 1011 (2011).